



Variations of fluid pressure within the subducting oceanic crust and slow earthquakes

Aitaro Kato,¹ Takashi Iidaka,¹ Ryoya Ikuta,² Yasuhiro Yoshida,³ Kei Katsumata,⁴ Takaya Iwasaki,¹ Shin'ichi Sakai,¹ Clifford Thurber,⁵ Noriko Tsumura,⁶ Koshun Yamaoka,⁷ Toshiki Watanabe,⁷ Takahiro Kunitomo,² Fumihito Yamazaki,⁷ Makoto Okubo,⁸ Sadaomi Suzuki,⁸ and Naoshi Hirata¹

Received 24 April 2010; revised 22 May 2010; accepted 1 June 2010; published 29 July 2010.

[1] We show fine-scale variations of seismic velocities and converted teleseismic waves that reveal the presence of zones of high-pressure fluids released by progressive metamorphic dehydration reactions in the subducting Philippine Sea plate in Tokai district, Japan. These zones have a strong correlation with the distribution of slow earthquakes, including long-term slow slip (LTSS) and low-frequency earthquakes (LFEs). Overpressured fluids in the LTSS region appear to be trapped within the oceanic crust by an impermeable cap rock in the fore-arc, and impede intraslab earthquakes therein. In contrast, fluid pressures are reduced in the LFE zone, which is deeper than the centroid of the LTSS, because there fluids are able to infiltrate into the narrow corner of the mantle wedge, leading to mantle serpentinization. The combination of fluids released from the subducting oceanic crust with heterogeneous fluid transport properties in the hanging wall generates variations of fluid pressures along the downgoing plate boundary, which in turn control the occurrence of slow earthquakes. **Citation:** Kato, A., et al. (2010), Variations of fluid pressure within the subducting oceanic crust and slow earthquakes, *Geophys. Res. Lett.*, 37, L14310, doi:10.1029/2010GL043723.

1. Introduction

[2] Slow earthquakes have been widely detected on the deep extension of megathrust faults around the circum-Pacific subduction zones [e.g., Obara, 2002; Ozawa et al., 2002; Rogers and Dragert, 2003; Kostoglodov et al., 2003; McCaffrey et al., 2008]. Because a slow earthquake is shear slip intermediate between fast, brittle rupture and slow, stable sliding [Ide et al., 2007], slow earthquakes effectively increase shear stress on the shallow dangerous megathrust faults. Recent studies of slow earthquakes point

to the involvement of high-pressure fluids near the plate boundary in the occurrence of slow earthquakes [Kodaira et al., 2004; Shelly et al., 2006; Liu and Rice, 2007; Audet et al., 2009; Song et al., 2009]. However, the geological origins and distributions of high pressured fluids are less well documented, even though this knowledge is likely to be crucially important in assessing the nature of slow earthquakes. Characterizing how and where high-pressure fluids are generated in association with ongoing subduction may help in understanding the temporal and spatial occurrence of slow earthquakes.

[3] The Philippine Sea Plate is subducting beneath the Eurasian Plate in a northwesterly direction through the Suruga trough in the Tokai district (Figure 1). Megathrust earthquakes with $M_w = 8$ have occurred persistently in the Tokai district with time intervals of approximately 150 years. Geodetic measurements have outlined the seismic gap as a strongly coupled area with slip deficit rate greater than 20 mm/yr [Ozawa et al., 2002; Suito and Ozawa, 2009]. Down-dip from the locked zone, a long-term slow slip (LTSS) occurred from 2000 to 2005, for which the cumulative moment magnitude reached 7.1 [Suito and Ozawa, 2009]. Additionally, slow earthquakes with shorter characteristic durations than the LTSS, represented by non-volcanic tremors, LFEs and short-term slow slips, have been detected near the down-dip edge of the LTSS area (Figure 1) [Hirose and Obara, 2006; Suda et al., 2009]. This lateral offset between the LTSS and the other slow earthquakes with shorter durations provides us a unique opportunity to elucidate effect of fluid pressures on the characteristic durations or dimensions of slow earthquakes.

[4] To investigate variations of seismic structure correlated with the slow earthquakes, we deployed a dense linear array in 2008 consisting of 80 temporary seismic stations with a length of 100 km extending from the locked to the aseismic stable sliding regime (Figure 1). We then merged this array data with data from permanent stations in the study region. High-resolution seismic tomography and receiver function techniques were used to image structural elements within the subduction complex as well as to determine precise hypocenter solutions, including LFEs.

2. Data and Methods

[5] The dense seismic observations were conducted from April to August in 2008 (Figure 1b). The linear array consists of 70 seismometers with 1 Hz natural frequency, 5 seismometers with 2 Hz natural frequency and 5 accelerometers, those continuously recorded three-component

¹Earthquake Research Institute, University of Tokyo, Tokyo, Japan.

²Department of Geosciences, Shizuoka University, Shizuoka, Japan.

³Meteorological Research Institute, Tsukuba, Japan.

⁴Institute of Seismology and Volcanology, Hokkaido University, Sapporo, Japan.

⁵Department of Geoscience, University of Wisconsin-Madison, Madison, Wisconsin, USA.

⁶Graduate School of Science, Chiba University, Chiba, Japan.

⁷Graduate School of Environmental Studies, Nagoya University, Nagoya, Japan.

⁸Tono Research Institute of Earthquake Science, Association for the Development of Earthquake Prediction, Mizunami, Japan.

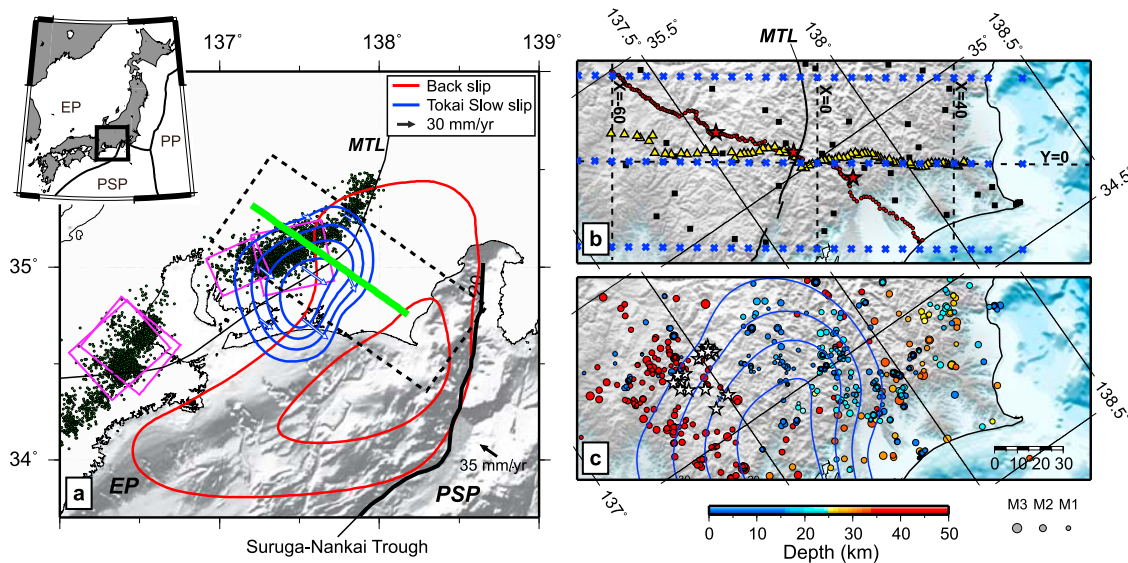


Figure 1. Seismotectonic setting of central Japan and locations of linear seismic array. (a) The linear seismic array subparallel to the convergence direction of the Philippine Sea plate (PSP) is denoted as a bold green line. Blue contour lines and arrows represent slip rate and slip direction of the long-term slow slip from 2000 to 2005, and red ones indicate slip deficit rate from 1997 to 1999 [Suito and Ozawa, 2009]. Contour lines for rates larger than 20 mm/yr are drawn with an interval of 10 mm/yr. Dots are LFE locations determined by the Japan Meteorological Agency (JMA). Purple rectangles show fault slip models of short term slow slip events [Hirose and Obara, 2006]. The dashed rectangle indicates the regional location of Figures 1b and 1c. The black arrow represents the direction of relative plate motion in the Tokai district [Sagiya, 1999]. MTL, Median Tectonic Line; EP, Eurasian plate; PP, Pacific plate. (b) Distributions of 80 portable seismic stations (yellow triangles) and grid nodes used in the tomographic analysis (blue crosses) plotted on the rotated map. Red circles are offline stations deployed during a seismic survey conducted in 2001 with three explosions (red stars) [Kodaira et al., 2004]. Solid squares denote permanent stations. (c) Relocated regular earthquakes as circles scaled to earthquake magnitude and color coded to depth. Open stars represent epicenters of LFEs relocated in the present study.

signals at a sampling rate of 200 or 100 Hz. Both P- and S-wave arrival times from 782 earthquakes including 17 LFEs were manually picked from waveforms observed by both dense temporary stations and permanent stations. Additionally, we used first arrival time data of three explosive sources recorded by 185 seismic stations deployed in 2001 along a seismic survey line [Kodaira et al., 2004].

[6] The double-difference tomography method [Zhang and Thurber, 2003] was then applied to the arrival time data. We used absolute arrival times with the differential arrival times for the manually picked and more accurate differential arrival times obtained by the waveform cross-correlation method. The grid spacing for the tomography ranges from 3 to 5 km on the depth section parallel to the seismic array profile. For details, please see Text S1 and Figures S1–S6 of the auxiliary material.¹

[7] We calculated receiver functions using teleseismic waveforms recorded by stations equipped with 1 Hz seismometers within the array, applying the spectral division [Ammon, 1991] method with a water level fraction of 0.01 and Gaussian filter width of 3.0 (~2 Hz low-pass filters) (Text S1 and Figure S7). The time series of the receiver functions were converted to depth sections applying a form of migration to each event-station pairing, where each receiver function is repositioned to the predicted location of the P - S converted phases assuming a one-dimensional velocity model for each station. The one-dimensional

velocity model beneath each station was constructed from interpolation of the final tomography model (Figure S4). The depth series of each receiver function can be represented by a bending ray with ray parameter and back-azimuth. The individual migrated receiver functions were then stacked onto 1 km by 1 km cells along the seismic array profile.

3. Results and Discussions

[8] A depth-section of receiver functions (Figure 2e) shows that the oceanic crust, of which the top and bottom (plate interface and oceanic Moho) are outlined by strong negative and positive amplitudes, respectively, is subducting at a dip angle of approximately 15°. The subducting oceanic crust is on average characterized by relatively low-velocities and high V_p/V_s ratios (Figures 2b–2d), interpreted to indicate fluids released by progressive metamorphic dehydration reactions in the oceanic crust [Hacker et al., 2003]. Extrapolation of laboratory measurements made at lower pressures [Christensen, 1984] allows us to interpret the velocity anomalies as variations of fluid pressures within the downgoing oceanic crust.

[9] Anomalous low V_p and V_s velocities with peak V_p/V_s ratio (~1.95) in the oceanic crust coincide with the centroid of the LTSS area. The area of anomalously low velocities corresponds to a subducted ridge imaged as a slightly upward doming structure of seismic reflectors by Kodaira et al. [2004]. The seismic velocities of the subducted ridge ($V_p \sim 6.6$ km/s, $V_s \sim 3.5$ km/s (see Figure S4)) are lower and V_p/V_s is higher than those of common oceanic crustal

¹Auxiliary materials are available in the HTML. doi:10.1029/2010GL043723.

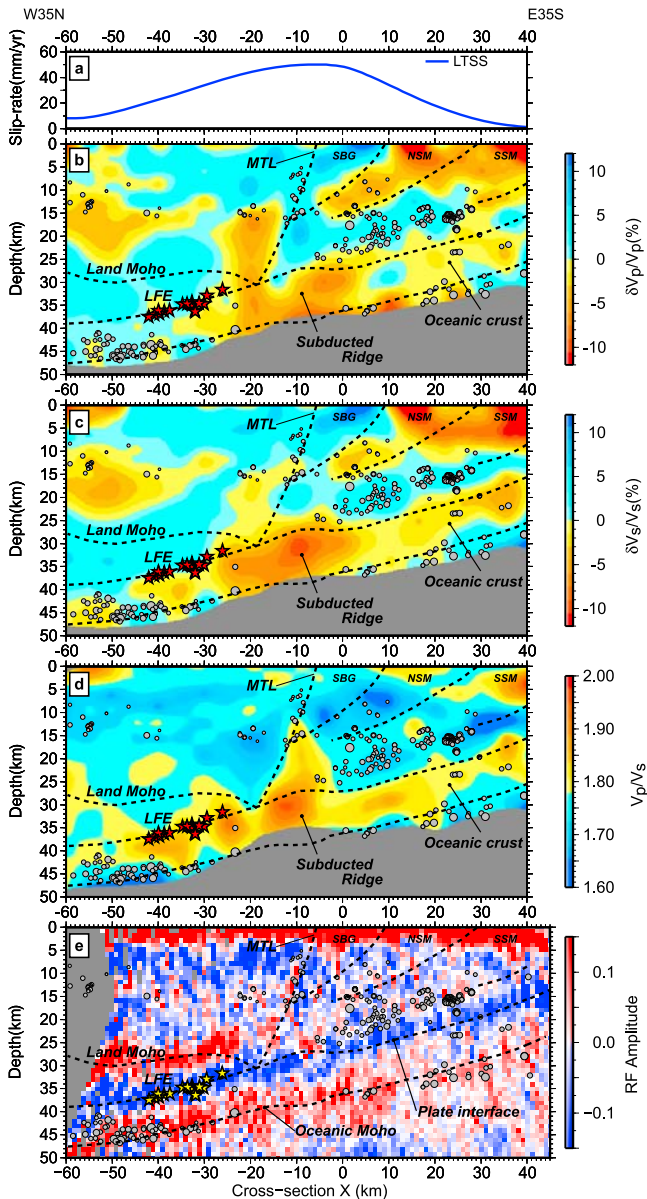


Figure 2. Depth sections of seismic velocities and receiver functions beneath the linear seismic array (along the section $Y = 0$). (a) Profile of slip rate of the long-term slow slip event (LTSS). (b) P-wave velocity perturbation $\delta V_p/V_p$. (c) S-wave velocity perturbation $\delta V_s/V_s$. (d) V_p/V_s ratio. (e) Receiver function results. Relocated hypocenters are plotted for events within 10 km of each cross-section with gray circles indicating regular earthquakes and red stars indicating LFEs. Gray-masked areas represent regions of poor resolution. Our interpretation of seismic structure is superimposed on each section. The contours of the subducting oceanic crust are drawn based on the receiver function image. SBG, Sanbagawa metamorphic belt; NSM, Northern Shimanto accretionary complex; SSM, Southern Shimanto accretionary complex.

rocks basalt (greenschist facies), diabase and gabbro [Hacker et al., 2003; Christensen, 1996].

[10] Intraslab earthquakes dipping parallel to the plate interface are distributed near the Moho of the subducting oceanic crust (Figure 2e). However, the intraslab seismicity

in the subducted ridge with anomalously low velocities is almost completely suppressed (Figure 3a). A commonly invoked mechanism to promote intraslab earthquakes is the dehydration embrittlement of serpentine within the slab [Kirby et al., 1996]. The kinetics of serpentine dehydration [Perrillat et al., 2005] indicates that overpressured (near lithostatic) fluids impede the dehydration reactions, which would in turn lead to a paucity of intraslab seismicity. As an alternative hypothesis, a local temperature increase near the subducted ridge could impede the intraslab seismicity. However, the thermal anomaly associated with the ridge may be less significant, because formation of the ridge is predominantly related to tectonic crustal shortening/thickening, based on the seismic images acquired in shallow portions of a zone of cyclic ridge subduction offshore the Tokai district [e.g., Mazzotti et al., 2002].

[11] Thus, the combination of the anomalously low-velocities and high- V_p/V_s ratio with the paucity of intraslab earthquakes is consistent with the inference that overpressured fluids are trapped within the subducted ridge. To generate overpressured fluids, it is necessary to seal pathways for fluid transport into the overlying fore-arc crust. Indeed, a high- V_p body with moderately high- V_p/V_s ratio is present (and was presumably underplated) at the base of the fore-arc crust ($-20 < X < 0$ km). This high- V_p body just above the overpressured subducted ridge is interpreted to act as an impermeable barrier or cap rock that restricts fluid movement and generates the fluid overpressure [Audet et al., 2009; Reyners and Eberhart-Phillips, 2009].

[12] At the greater depths of the LTSS area ($-45 < X < -25$ km), well relocated LFEs align linearly along the plate interface at the onset of the contact between the mantle wedge corner (i.e., the base of the land Moho as delineated by a positive amplitude in the receiver functions) and the top of the oceanic crust. The underlying oceanic crust is characterized by slightly reduced velocities and moderately high V_p/V_s ratio (~ 1.85), which implies that high-pressure fluids are still present. However, the amplitudes of the seismic anomalies are diminished compared with those of the subducted ridge (LTSS centroid area) (Figures 2 and 3b). We therefore infer that fluid pressures within the oceanic crust are somewhat reduced in the LFE zone. This fluid pressure reduction is likely to be caused by partial leakage of fluids into the overlying mantle wedge corner. If fluids infiltrate into anhydrous mantle, mantle serpentinization occurs [e.g., Bostock et al., 2002; Kawakatsu and Watada, 2007]. Indeed, the mantle wedge above the LFE alignment has lower velocities ($V_p \sim 7.2$ km/s, $V_s \sim 4.0$ km/s), and moderately high V_p/V_s ratio (~ 1.8) compared to typical anhydrous mantle (Figure S4). The amount of velocity reductions indicates 20–30% serpentinization in the mantle wedge [Hyndman and Peacock, 2003]. Beneath the Tokai, serpentinization of the mantle wedge has not progressed to the point of producing an inverted Moho as observed in the Cascadia subduction zone [Bostock et al., 2002]. Since non-volcanic tremor is largely composed of swarms of LFEs in SW Japan [Shelly et al., 2007], it is expected that tremors should also occur along the plate interface beneath the serpentinized mantle wedge. It is worth noting that our results provide new evidence documenting the spatial relationship between tremors and serpentinized mantle.

[13] At the lowermost imaged depth of the oceanic crust ($-60 < X < -45$ km), the oceanic crust shows a rapid

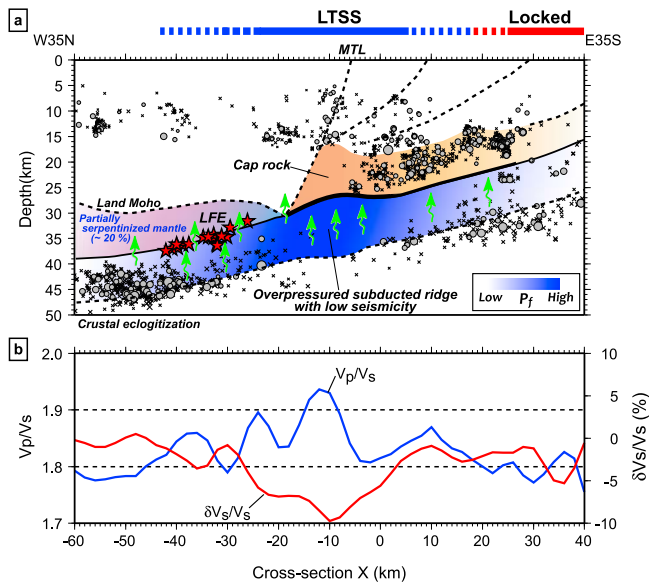


Figure 3. Schematic interpretations of seismic structures. (a) Fluid pressures P_f within the subducting oceanic crust are color coded to magnitude. Green arrows denote potential fluid pathways in the subduction zone. Gray circles are relocated earthquakes observed by the linear array. Crosses represent earthquakes from 2003 to 2007 relocated in the final velocity model (Text S1 and Figure S4). (b) Variations of $\delta V_s/V_s$ and V_p/V_s ratio within the subducting oceanic crust.

reduction of V_p/V_s ratio and an increase of seismic velocities accompanied by abundant intraslab earthquakes. These intraslab earthquakes are occurring in a normal faulting stress regime [Toda and Matsumura, 2006] and cease approximately 10 km northwestward ($X \sim -70$ km). Furthermore, the Philippine Sea slab appears to initiate its downward bend at approximately 50 km depth based on a regional large-scale tomography model [Nakajima and Hasegawa, 2007]. We interpret these observations as indicating the onset of eclogitization of the oceanic crust, which corresponds to a phase transformation of hydrous minerals in basalt from epidote-blueschist to amphibole-eclogite facies. The fluids released by the eclogitization further enhance the serpentinization of the mantle wedge and LFEs.

[14] At the shallower depths of the LTSS area ($5 < X < 30$ km), we infer that fluid pressures within the oceanic crust are further reduced compared with those of the LFE zone, based on decrease in amplitudes of the seismic anomalies (Figure 2). This fluid pressure reduction is likely caused by low production rate of fluids in low temperature conditions. The base of the fore-arc crust, which is characterized by high-velocities with low V_p/V_s ratio dipping parallel to the subducting oceanic crust, is also interpreted to act as the cap rock.

[15] We find a vertically elongated low velocity zone at the northwest side of the deep extension of the Median Tectonic Line (MTL) (Figure 2). This low-velocity anomaly with low- V_p/V_s ratio appears to originate from the plate boundary. According to Takei [2002], the low- V_p/V_s ratio as well as the low-velocities can be explained by the presence of fluid-filled pores with high aspect ratios (~ 0.1). It thus seems probable that some fluids leaking from the overpressured subducted ridge migrate upward along deep shear

zones of the MTL, which function as fluid conduits. Fluids reduce the strength of crustal rocks, enhancing ductile creep [Carter and Tsenn, 1987], so weak shear zones could develop at the deep extension of the MTL, which in turn leads to loading on brittle faults in the upper crust. This implies that deep subduction fluids can induce crustal seismogenesis [Wannamaker et al., 2009]. One may argue that if fluids are able to migrate along the MTL, it would be difficult to maintain the high fluid pressure within the subducting oceanic crust at depths greater than the MTL contact. However, it is possible that crustal eclogitization supplies additional fluids to help maintain the high fluid pressure.

[16] The present results suggest that combination of dehydration fluids with heterogeneous fluid transport properties in the overlying fore-arc plate generates variations of fluid pressures along the downgoing plate boundary, which in turn control the occurrence of slow earthquakes. Focusing around the centroid of the LTSS area, inferred fluid pressures within the subducting oceanic crust gradually decrease both updip and downdip (Figure 3), but in an asymmetric manner: higher pressure appears to extend further downdip than updip. This asymmetric distribution of fluid pressures correlates well with the slip-rate of the LTSS (Figure 2a).

[17] Our results that the fluid pressure in the centroid of the LTSS is larger than that of the LFE zone imply that as fluid pressure increases, the characteristic dimension of the fault plane L of a slow earthquake increases. Therefore, it is plausible that stress drop $\Delta\sigma$ released by a slow earthquake decrease as L increases, because $\Delta\sigma$ associated with quasi-static shear slip is likely to be proportional to the effective normal stress. This inverse dependence of $\Delta\sigma$ on L indicates that a diffusional earthquake model [Ide et al., 2007] involving high-pressure fluids is preferable as the basic mechanism of slow earthquakes.

4. Conclusions

[18] Based on fine-scale variations of seismic velocities and converted teleseismic waves, we reveal that the combination of fluids released from the subducting oceanic crust with heterogeneous fluid transport properties in the hanging wall (i.e., a cap rock at the base of the overlying plate and mantle wedge corner) generates variations of fluid pressure along the plate boundary. Focusing around the centroid of the LTSS area, inferred fluid pressures within the subducting oceanic crust gradually decrease both updip and downdip, but in an asymmetric manner: higher pressure appears to extend further downdip, where tremors or LFEs are present, than updip. This asymmetric distribution of fluid pressures correlates well with the slip-rate of the LTSS.

[19] **Acknowledgments.** We are thankful to H. Zhang for allowing us to use the TomoDD code. We thank T. Igarashi, H. Sato, S. Ide, and an anonymous reviewer for useful comments and suggestions. We are grateful to K. Nozaki and F. Takahashi for data acquisition. We thank NIED and JMA for allowing us to use waveform data collected from their permanent stations. JMA provided us with the earthquake catalog.

References

Ammon, C. J. (1991), The isolation of receiver function effect from teleseismic P waveforms, *Bull. Seismol. Soc. Am.*, *81*, 2504–2510.

- Audet, P., M. G. Bostock, N. I. Christensen, and S. M. Peacock (2009), Seismic evidence for overpressured subducted oceanic crust and megathrust fault sealing, *Nature*, *457*, 76–78, doi:10.1038/nature07650.
- Bostock, M., R. D. Hyndman, S. Rondenay, and S. M. Peacock (2002), An inverted continental Moho and serpentinization of the forearc mantle, *Nature*, *417*, 536–538, doi:10.1038/417536a.
- Carter, N. L., and M. C. Tsenn (1987), Flow properties of the continental lithosphere, *Tectonophysics*, *136*, 27–63, doi:10.1016/0040-1951(87)90333-7.
- Christensen, N. I. (1984), Pore pressure and oceanic crustal seismic structure, *Geophys. J. R. Astron. Soc.*, *79*, 411–423.
- Christensen, N. I. (1996), Poisson's ratio and crustal seismology, *J. Geophys. Res.*, *101*, 3139–3156, doi:10.1029/95JB03446.
- Hacker, B. R., G. A. Abers, and S. M. Peacock (2003), Subduction factory: 1. Theoretical mineralogy, densities, seismic wave speeds, and H₂O contents, *J. Geophys. Res.*, *108*(B1), 2029, doi:10.1029/2001JB001127.
- Hirose, H., and K. Obara (2006), Short-term slow slip and correlated tremor episodes in the Tokai region, central Japan, *Geophys. Res. Lett.*, *33*, L17311, doi:10.1029/2006GL026579.
- Hyndman, R. D., and S. M. Peacock (2003), Serpentinization of the forearc mantle, *Earth Planet. Sci. Lett.*, *212*, 417–432, doi:10.1016/S0012-821X(03)00263-2.
- Ide, S., G. C. Beroza, D. R. Shelly, and T. Uchide (2007), A scaling law for slow earthquakes, *Nature*, *447*, 76–79, doi:10.1038/nature05780.
- Kawakatsu, H., and S. Watada (2007), Seismic evidence for deep-water transportation in the mantle, *Science*, *316*, 1468–1471, doi:10.1126/science.1140855.
- Kirby, S., E. R. Engdahl, and R. Denlinger (1996), Intermediate-depth, intraslab earthquakes and arc volcanism as physical expressions of crustal and uppermost mantle metamorphism in subducting slabs (overview), in *Subduction: Top to Bottom*, *Geophys. Monogr. Ser.*, vol. 96, edited by G. E. Bebout et al., pp. 195–214, AGU, Washington, D. C.
- Kodaira, S., T. Iidaka, A. Kato, J.-O. Park, T. Iwasaki, and Y. Kaneda (2004), High pore fluid pressure may cause silent slip in the Nankai Trough, *Science*, *304*, 1295–1298, doi:10.1126/science.1096535.
- Kostoglodov, V., S. K. Singh, J. A. Santiago, S. I. Franco, K. M. Larson, A. R. Lowry, and R. Bilham (2003), A large silent earthquake in the Guerrero seismic gap, Mexico, *Geophys. Res. Lett.*, *30*(15), 1807, doi:10.1029/2003GL017219.
- Liu, Y., and J. R. Rice (2007), Spontaneous and triggered aseismic deformation transients in a subduction fault model, *J. Geophys. Res.*, *112*, B09404, doi:10.1029/2007JB004930.
- Mazzotti, S., S. Lallemand, P. Henry, X. Le Pichon, H. Tokuyama, and N. Takahashi (2002), Intraplate shortening and underthrusting of a large basement ridge in the eastern Nankai subduction zone, *Mar. Geol.*, *187*, 63–88, doi:10.1016/S0025-3227(02)00245-1.
- McCaffrey, R., L. M. Wallace, and J. Bevan (2008), Slow slip and frictional transition at low temperature at the Hikurangi subduction zone, *Nat. Geosci.*, *1*, 316–320, doi:10.1038/ngeo178.
- Nakajima, J., and A. Hasegawa (2007), Subduction of the Philippine Sea plate beneath southwestern Japan: Slab geometry and its relationship to arc magmatism, *J. Geophys. Res.*, *112*, B08306, doi:10.1029/2006JB004770.
- Obara, K. (2002), Nonvolcanic deep tremor associated with subduction in southwest Japan, *Science*, *296*, 1679–1681, doi:10.1126/science.1070378.
- Ozawa, S., M. Murakami, M. Kaidzu, T. Tada, T. Sagiya, Y. Hatanaka, H. Yurai, and T. Nishimura (2002), Detection and monitoring of ongoing aseismic slip in the Tokai region, central Japan, *Science*, *298*, 1009–1012, doi:10.1126/science.1076780.
- Perrillat, J.-P., I. Daniel, K. T. Koga, B. Reynard, H. Cardon, and W. A. Crichton (2005), Kinetics of antigorite dehydration: A real-time X-ray diffraction study, *Earth Planet. Sci. Lett.*, *236*, 899–913, doi:10.1016/j.epsl.2005.06.006.
- Reyners, M., and D. Eberhart-Phillips (2009), Small earthquakes provide insight into plate coupling and fluid distribution in the Hikurangi subduction zone, New Zealand, *Earth Planet. Sci. Lett.*, *282*, 299–305, doi:10.1016/j.epsl.2009.03.034.
- Rogers, G., and H. Dragert (2003), Episodic tremor and slip on the Cascadia subduction zone: The chatter of silent slip, *Science*, *300*, 1942–1943, doi:10.1126/science.1084783.
- Sagiya, T. (1999), Interplate coupling in the Tokai district, central Japan, deduced from continuous GPS data, *Geophys. Res. Lett.*, *26*, 2315–2318, doi:10.1029/1999GL900511.
- Shelly, D. R., G. C. Beroza, and S. Ide (2006), Low-frequency earthquakes in Shikoku, Japan, and their relationship to episodic tremor and slip, *Nature*, *442*, 188–191, doi:10.1038/nature04931.
- Shelly, D. R., G. C. Beroza, and S. Ide (2007), Non-volcanic tremor and low frequency earthquake swarms, *Nature*, *446*, 305–307, doi:10.1038/nature05666.
- Song, T.-R. A., D. V. Helmberger, M. R. Brudzinski, R. W. Clayton, P. Davis, X. Perez-Campos, and S. K. Singh (2009), Subducting slab ultra-slow velocity layer coincident with silent earthquakes in southern Mexico, *Science*, *324*, 502–506.
- Suda, N., R. Nakata, and T. Kusumi (2009), An automatic monitoring system for nonvolcanic tremors in southwest Japan, *J. Geophys. Res.*, *114*, B00A10, doi:10.1029/2008JB006060.
- Suito, H., and T. Ozawa (2009), Transient crustal deformation in the Tokai district, *J. Seismol. Soc. Jpn.*, *2*(61), 113–135.
- Takei, Y. (2002), Effect of pore geometry on VP/VS: From equilibrium geometry to crack, *J. Geophys. Res.*, *107*(B2), 2043, doi:10.1029/2001JB000522.
- Toda, S., and S. Matsumura (2006), Spatial-temporal stress states estimated from seismicity rate changes in the Tokai region, central Japan, *Tectonophysics*, *417*, 53–68, doi:10.1016/j.tecto.2005.08.030.
- Wannamaker, P., T. G. Caldwell, G. R. Jiracek, V. Maris, G. J. Hill, Y. Ogawa, H. M. Bibby, S. L. Bennie, and W. Heise (2009), Fluid and deformation regime of an advancing subduction system at Marlborough, New Zealand, *Nature*, *460*, 733–736, doi:10.1038/nature08204.
- Zhang, H., and C. H. Thurber (2003), Double-difference tomography: The method and its application to the Hayward fault, California, *Bull. Seismol. Soc. Am.*, *93*, 1875–1889, doi:10.1785/0120020190.
- N. Hirata, T. Iidaka, T. Iwasaki, A. Kato, and S. Sakai, Earthquake Research Institute, University of Tokyo, 1-1-1 Yayoi, Bunkyo-ku, Tokyo 113-0032, Japan. (akato@eri.u-tokyo.ac.jp)
- R. Ikuta and T. Kunitomo, Department of Geosciences, Shizuoka University, 836 Ohya, Shizuoka 422-8529, Japan.
- K. Katsumata, Institute of Seismology and Volcanology, Hokkaido University, North-10, West-8, Sapporo 060-0810, Japan.
- M. Okubo and S. Suzuki, Tono Research Institute of Earthquake Science, Association for the Development of Earthquake Prediction, 1-63 Yamanouchi, Akeyo, Mizunami, Gifu 509-6132, Japan.
- C. Thurber, Department of Geoscience, University of Wisconsin-Madison, 1215 W. Dayton St., Madison, WI 53706, USA.
- N. Tsumura, Graduate School of Science, Chiba University, Yayoi-cho 1-33, Inage-ku, Chiba 263-8522, Japan.
- T. Watanabe, K. Yamaoka, and F. Yamazaki, Graduate School of Environmental Studies, Nagoya University, Furo-cho, Chikusa-ku, Nagoya 464-8601, Japan.
- Y. Yoshida, Meteorological Research Institute, Nagamine 1-1, Tsukuba, Ibaraki 305-0052, Japan.